Proc. Natl. Acad. Sci. USA
Vol. 96, pp. 5251–5256, April 1999
Neurobiology

Mutually exclusive expression of human red and green visual pigment-reporter transgenes occurs at high frequency in murine cone photoreceptors

YANSHU WANG*, PHILIP M. SMALLWOOD*†, MITRA COWAN‡, DIANE BLESH‡, ANN LAWLER§, AND JEREMY NATHANS*†¶‖**

*Department of Molecular Biology and Genetics, ¶Department of Neuroscience, ‖Department of Ophthalmology, †Howard Hughes Medical Institute, ‡Transgenic Core Facility, and §Department of Gynecology and Obstetrics, Johns Hopkins University School of Medicine, Baltimore, MD 21205

Contributed by Jeremy Nathans, February 19, 1999

ABSTRACT **This study examines the mechanism of mutually exclusive expression of the human X-linked red and green visual pigment genes in their respective cone photoreceptors by asking whether this expression pattern can be produced in a mammal that normally carries only a single X-linked visual pigment gene. To address this question, we generated transgenic mice that carry a single copy of a minimal human X chromosome visual pigment gene array in which the red and green pigment gene transcription units were replaced, respectively, by alkaline phosphatase and β-galactosidase reporters. As determined by histochemical staining, the reporters are expressed exclusively in cone photoreceptor cells. In 20 transgenic mice carrying any one of three independent transgene insertion events, an average of 63% of expressing cones have alkaline phosphatase activity, 10% have β-galactosidase activity, and 27% have activity for both reporters. Thus, mutually exclusive expression of red and green pigment transgenes can be achieved in a large fraction of cones in a dichromat mammal, suggesting a facile evolutionary path for the development of trichromacy after visual pigment gene duplication. These observations are consistent with a model of visual pigment expression in which stochastic pairing occurs between a locus control region and either the red or the green pigment gene promotor.**

Humans and a subset of nonhuman primates have trichromatic color vision, whereas other mammals have dichromatic color vision (1). In humans, three genes code for the visual pigments that mediate color vision. The red (long-wave) and green (middle-wave) pigments are coded on the X chromosome by nearly identical genes that are the products of a duplication that occurred within the primate lineage, approximately 30–40 million years ago. The blue (short-wave) pigment is coded by an autosomal gene that split from the ancestral red/green pigment gene before the vertebrate radiation. Psychophysical, microspectrophotometric, and electrophysiologic studies of the primate retina indicate that cone pigment genes are expressed in a mutually exclusive manner in their respective cone photoreceptors (2–4).

The relatively short time that has elapsed since the duplication of red and green pigment genes suggests a corresponding simplicity in the possible mechanisms that could have evolved to generate their mutually exclusive pattern of expression. We consider below two general classes of mechanisms or models that could account for this pattern. One model, which we will refer to as the "standard" model, envisions the choice of red or green pigment gene transcription to result from the differential binding of red or green cone-specific transcriptional regulatory proteins to DNA sequences adjacent to the red and green pigment genes. The existence of transcription factors specific to red or green cones could also lead to the differential expression of other genes that might distinguish these cells, in particular genes involved in determining the specificity of synaptic connections. An alternate model, which we will refer to as the "stochastic" model, assumes that red and green cones contain identical transcriptional regulatory proteins. In this model, the choice of red or green pigment gene transcription is envisioned to result from a stochastic choice between alternative configurations of cis-acting DNA sequences and their associated proteins such that a stable transcription complex forms on only one visual pigment gene promotor in the X chromosome array. In the simplest version of the stochastic model, the choice of red or green pigment gene expression is presumed to exert no influence on the expression of other genes, implying that red and green cones possess no molecular differences other than the pigments they contain. If correct, the simple version of the stochastic model would also imply that at more distal stages of visual processing red and green cone signals are only distinguishable by Hebbian mechanisms (i.e., those based on correlated activity).

One specific mechanism that could account for the stochastic model has been proposed based on the existence of a locus control region (LCR) adjacent to the visual pigment gene array (5, 6). The LCR was originally defined as a DNA segment between 3.1 and 3.7 kb 5′ of the red pigment gene promotor that is required in humans for the activity of all visual pigment genes in the array (5). Earlier transgenic mouse experiments demonstrated that both the LCR and a visual pigment promotor are required for cone-specific expression of a transgene containing a β-galactosidase (β-gal) reporter. Either removing the LCR or replacing the visual pigment promotor with a herpes simplex virus thymidine kinase (HSV TK) minimal promoter results in a complete loss of transgene expression (ref. 6; Y.W. and J.N., unpublished data). The DNA sequence of the LCR is highly conserved across mammals and appears not to have been duplicated in those primates with trichromatic color vision. This observation suggests that in all mammals, the LCR interacts with a single visual pigment gene promotor and thereby activates transcription from that gene alone (6).

To distinguish between the two competing models, we asked whether a mammal that normally possesses only a single X chromosome-linked visual pigment gene could support mutu-

Abbreviations: AP, alkaline phosphatase; β-gal, β-galactosidase; TK, thymidine kinase; NBT, nitroblue tetrazolium; X-Gal, 5-bromo-4-chloro-3-indolyl β-D-galactopyranoside; X-phos, 5-bromo-4-chloro-3-indolyl phosphate; LCR, locus control region; HSV TK, herpes simplex virus thymidine kinase; PGK, phosphoglycerate kinase.

A Commentary on this article begins on page 4743.

**To whom reprint requests should be addressed at 805 Preclinical Teaching Building, 725 North Wolfe Street, Johns Hopkins University School of Medicine, Baltimore, MD 21205. e-mail: jnathans@jhmi.edu.

The publication costs of this article were defrayed in part by page charge payment. This article must therefore be hereby marked "*advertisement*" in accordance with 18 U.S.C. §1734 solely to indicate this fact.

PNAS is available online at www.pnas.org.

ally exclusive expression of the human red and green pigment genes when these are integrated into its genome. The standard model predicts that only primates with trichromatic color vision have evolved the requisite transcriptional regulators to distinguish red and green pigment genes, whereas the stochastic model predicts that the red-vs.-green choice is effected by transcriptional regulators common to all mammals. We therefore generated transgenic mice carrying a single copy of a minimal human X chromosome visual pigment gene array in which the red and green pigment gene transcription units and 3′ intergenic sequences were replaced by alkaline phosphatase (AP) and β-gal reporters, respectively, and then determined the expression patterns of the two reporters in the retina.

MATERIALS AND METHODS

Embryonic Stem Cells and Blastocyst Injection. R1 cells (a gift of Janet Rossant, Mount Sinai Hospital, Toronto and Se-jin Lee, Johns Hopkins University School of Medicine) were electroporated with the minimal array construct linearized at a unique *Not*I site immediately 5′ of the LCR, and colonies were selected in G418. Colonies (184) were screened by Southern blot hybridization: *Eco*RI + *Hin*dIII digests were hybridized with a probe derived from the mouse protamine 1 gene (present at the 3′ end of each reporter casette) to determine the copy number of the transgene array, and 44 of these were subsequently hybridized with a probe derived from the LCR to confirm the integrity of the 5′ end of the array. Six embryonic stem cell colonies were judged to carry single, unrearranged transgenic arrays and of these, three (1A3, 1G11, and 2G10) were injected into blastocysts to derive chimeric mice.

Histochemistry. 5-Bromo-4-chloro-3-indolyl β-D-galactopyranoside (X-Gal) and 5-bromo-4-chloro-3-indolyl phosphate/nitroblue tetrazolium (X-phos/NBT) histochemical reactions were performed essentially as described (6, 7) after brief gluteraldehyde fixation of eye cups or isolated retinas. X-Gal staining was performed for 1–2 days at 37°C, and the tissue was further fixed, heated to 65°C to eliminate endogenous AP activity, stained with X-phos/NBT, cryoprotected in sucrose, frozen in OCT, and sectioned. In some cases the tissue was sectioned before the X-phos/NBT reaction.

Kinetic Model for Switching Between Reporters. For the kinetic model, all cells are assumed to express only a single reporter at any time and double labeled cells are assumed to reflect the perdurance of previously expressed reporter mRNA and protein. At steady state, a 6-fold excess of AP-expressing cells over β-gal-expressing cells implies that the rate constant for switching from AP to β-gal is one-sixth that of the reverse rate constant. The switching process can be envisioned as an occasional dissolution of the active transcription complex, followed by reassembly of an active complex with a 6-fold bias in favor of assembly at the red pigment promoter. If the perdurance of the two reporters is assumed to be equal and is X days then, by definition, all cones that have switched within the preceding X days will be double-labeled and all cones that have not switched during the preceding X days will be single-labeled. If switching is assumed to be a stochastic event, then for each cone, the probability that no switches will have occurred over time t is $P(\text{no switches}) = e^{-kt}$, where k defines the switching frequency. If F represents the fraction of cones that are singly labeled at steady state, then $F = e^{-kX}$. For F = 0.75 and X = 5 days, we obtain k = 0.0575. Setting P(no switches) = 0.5, and using k = 0.0575, we obtain $t_{1/2}$ = 12 days.

RESULTS

Generation of Mice Carrying a Single Visual Pigment-Reporter Array. The minimal X-linked visual pigment gene array (Fig. 1) contains a 0.5-kb segment encompassing sequences immediately 5′ of the red pigment gene transcription start site (referred to hereafter as the red pigment gene promoter) linked to a human placental AP reporter cassette (8) followed by a 0.5-kb segment encompassing sequences immediately 5′ of the green pigment gene transcription start site (referred to hereafter as the green pigment gene promoter) linked to an *Escherichia coli* β-gal reporter cassette (9). At its 5′ end, the minimal array carries the visual pigment LCR. A neomycin resistance gene driven by the phosphoglycerate kinase (PGK) promoter (10) and a HSV TK gene driven by a hybrid polyoma virus–HSV TK promoter (11, 12) are appended at the 3′ end of the minimal array. All transcription units within the transgene construct are oriented in the same direction as indicated in Fig. 1.

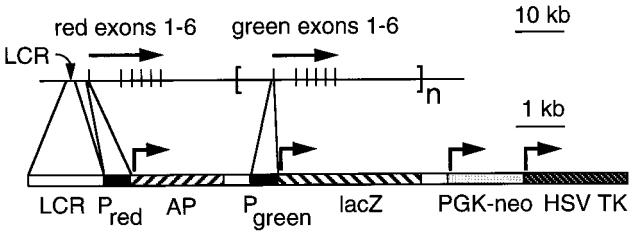

FIG. 1. Structure of a minimal human red/green visual pigment gene array in which the red pigment gene promotor controls transcription of an AP reporter and the green pigment gene promotor controls transcription of a β-gal reporter. The upper map shows the human X chromosome visual pigment gene array with the direction of transcription indicated by arrows and the six exons of each gene indicated by vertical lines (36–38). The LCR, defined by deletion mutations in blue cone monochromats (5) and by transgenic mouse experiments (6), is located between 3.1 and 3.7 kb 5′ of the start site of transcription of the red pigment gene. The lower map, at a 10-fold enlarged scale, shows the transgene construct which contains the following DNA segments, begining at the 5′ end: a *Bam*HI–*Stu*I fragment encompassing bases −4,564 to −3,009 5′ of the red pigment translation start site (LCR); a *Bam*HI–*Nco*I fragment encompassing 496 bases 5′ of the red pigment gene initiator methionine codon (P_{red}, the red pigment gene promotor and 5′-untranslated region); a human placental AP-coding region (AP; ref. 8); the mouse protamine gene intron and 3′-untranslated region (open box; ref. 9); a PCR fragment (verified by sequencing) encompassing 496 bases 5′ of the green pigment gene initiator methionine codon (P_{green}, the green pigment gene promotor and 5′-untranslated region); an *E. coli* β-gal-coding region (lacZ; ref. 9); the mouse protamine gene intron and 3′-untranslated region (open box); a PGK-neomycin resistance cassette (PGK-neo; ref. 10); and a pMC1-HSV TK cassette (11, 12). The arrows indicate the start site and direction of transcription.

To obtain single-copy integrants, the minimal array was electroporated into embryonic stem cells, and the resulting G418-resistant colonies were screened by Southern blotting to assess the copy number and integrity of the array. Of 184 colonies examined, 6 were judged to carry a single intact copy of the minimal array, and 3 of these were subsequently used to produce chimeric mice by blastocyst injection. Retinas from 20 of 43 chimeric mice proved suitable for quantitative analysis using the histochemical substrates X-Gal and X-phos/NBT for detection of β-gal and AP, respectively (Table 1).

Expression of the Transgenic Visual Pigment Gene Array. As expected, transgene expression was confined to cone photoreceptors as determined by morphology (6). A variable fraction of cones show transgene expression, presumably because of a combination of position effect variegation, as observed previously with other visual pigment transgenes (6, 13, 14), and tissue chimerism. We estimate that the histochemically detectable activity for each enzyme spans approximately a 10-fold range. Among cones that show histochemical staining, the majority stain only with X-Gal (10 ± 5%) or with X-phos/NBT (63 ± 15%), but not with both (Fig. 2 and Table 1). A subset of cones, ranging from 8% to 48% in different

Table 1. Histochemical analysis of reporter enzymes in transgenic mouse retinae

Origin of each retina			No. of cones in each class (% of total)		
Embryonic stem cell line	Mouse	Eye	$AP^+/\beta\text{-gal}^-$	$AP^-/\beta\text{-gal}^+$	$AP^+/\beta\text{-gal}^+$
1G11	2	1	1335 (67)	222 (11)	423 (21)
		2	2833 (71)	310 (8)	821 (21)
1G11	3	1	920 (76)	143 (12)	142 (12)
1G11	4	1	2538 (78)	301 (9)	405 (12)
		2	2704 (87)	133 (4)	255 (8)
2G10	6	1	263 (70)	24 (6)	91 (24)
1A3	7	1	336 (82)	14 (3)	60 (15)
		2	242 (83)	17 (6)	32 (11)
1A3	8	1	365 (60)	160 (26)	82 (14)
		2	1953 (80)	90 (4)	390 (16)
2G10	9	1	1087 (64)	239 (14)	374 (22)
2G10	10	1	2009 (66)	329 (11)	725 (24)
2G10	11	1	601 (34)	334 (19)	856 (48)
2G10	12	1	1176 (48)	184 (8)	1090 (44)
		2	955 (71)	83 (6)	308 (23)
2G10	14	1	406 (55)	76 (10)	253 (34)
		2	638 (69)	47 (5)	239 (26)
2G10	15	1	668 (47)	154 (11)	602 (42)
		2	808 (57)	84 (6)	521 (37)
2G10	18	1	835 (36)	434 (19)	1057 (45)
2G10	19	1	406 (42)	138 (14)	415 (43)
2G10	20	1	1404 (78)	34 (2)	372 (21)
2G10	22	1	1324 (70)	142 (7)	435 (23)
2G10	24	1	955 (67)	111 (8)	350 (25)
2G10	28	1	785 (57)	69 (5)	535 (39)
1A3	30	1	1184 (77)	142 (9)	218 (14)
1A3	33	1	937 (49)	295 (15)	688 (36)
Each animal weighted equally (mean ± S.D., %)			63 ± 14	10 ± 5	27 ± 12

Individual cones were counted in 10- to 15-μm sections after histochemical staining with X-gal and X-phos/NBT (see *Materials and Methods*). Among different cones within a single retina, the detectable intensity of each histochemical stain encompassed a range of approximately 10-fold. Cones that were scored as doubly labeled included examples that spanned the full range of detectable intensities and ratios of intensities for the two markers. In most cases, the number of cones counted represents only a fraction of the total number of stained cones in the retina. Of 43 chimeric mice examined, counts of histochemically stained cones were not obtained on 23 either because there were too few stained cells (14 mice), because the density of stained cells was too high (1 mouse), or because the quality of the fixation or histochemical reaction was judged to be poor (8 mice). Individual percentages have been rounded to the nearest whole number and therefore do not always sum to 100. The 45,938 cells reported in the table were scored by one person (Y.W.). Of all cells scored by Y.W., 4,349 were compared to 2,339 stained cells from the same animals scored by a second person (J.N.). The average difference in the two sets of scores is +6% for $AP^+/\beta\text{-gal}^-$, +7% for $AP^-/\beta\text{-gal}^+$, and −14% for $AP^+/\beta\text{-gal}^+$, with J.N. scoring more cones as singly labeled and fewer as doubly labeled. We note that selection in embryonic stem cells for expression of the *neo* gene most likely selected for integration events at chromosomal locations that were generally permissive for gene activity. The presence of the HSV TK cassette in the transgene construct precluded transmission through the male germ line and production of transgenic lines (35). Equally weighted animal values given as mean ± SD%.

retinas with a mean of 27 ± 12%, stain with both X-Gal and X-phos/NBT (Table 1). The different intracellular distributions of β-gal (a cytoplasmic protein) and AP (a plasma membrane protein) favor the identification of doubly labeled cells over the full range of detectable enzyme activity ratios. The X-Gal only, X-phos/NBT only, and X-Gal + X-phos/NBT stained cones are indistinguishable morphologically and

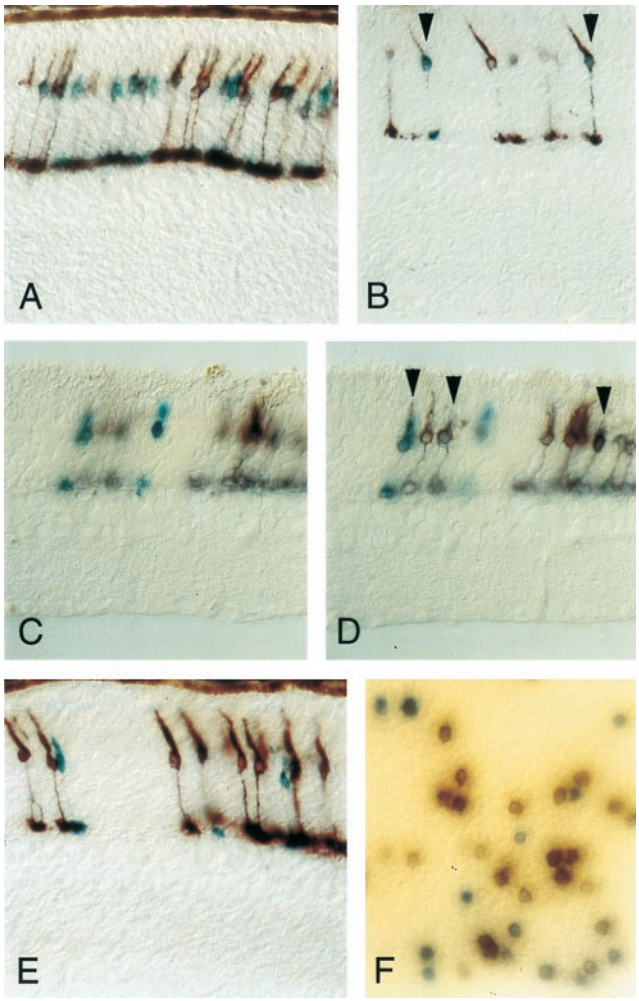

FIG. 2. Histochemical visualization of reporter enzyme activities in transgenic mouse retinae. Retinal sections 10–15 μm thick (A–*E*) and retinal flat mount (*F*) double-stained with X-Gal (blue reaction product) and X-phos/NBT (purple reaction product). In *A–E*, the full thickness of the retina is shown with the ganglion cell layer at the bottom of each panel. In *A*, *B*, and *E*, the tissue was processed with the retina and choroid attached; in *C* and *D*, the retina was dissected before histochemical processing. *C* and *D* show the same region of retina at different focal planes. Vertical arrows in *B* and *D* mark examples of double-stained cells: in *D*, the cell on the left has a greater level of X-Gal than X-phos/NBT staining, and the two other cells have greater levels of X-phos/NBT than X-Gal staining.

appear to be randomly intermingled among one another (Fig. 2). These data indicate that a large fraction of cone photoreceptors in the mouse retina can efficiently and selectively express either of the reporter transgenes within the minimal array, a result that strongly favors the stochastic model.

The 6-fold higher average frequency of X-phos/NBT over X-Gal-stained cones could arise from the greater proximity of the red promoter–AP reporter to the LCR or from an inherently greater efficiency of activation of the red promoter. This difference could also reflect, at least in part, a higher level of accumulation of AP relative to β-gal or a greater sensitivity of X-phos/NBT relative to X-Gal histochemistry. The idea that proximity to the LCR determines expression level has been advanced previously to explain the unequal expression of different green and/or hybrid pigment genes in retinae from subjects with three or more genes per array, although in those studies the order of the genes within the array was not known (15–17).

Doubly labeled cones could arise from simultaneous expression of both AP and β-gal reporters or they could arise from

an occasional switch between expression of one reporter and the other. With respect to the latter possibility, a simple calculation shows that if, at steady state, 25% of cells are double-labeled and the perdurance of detectable enzyme activity is X days, then the half-time ($t_{1/2}$) for switching is 2.4X days if switching is assumed to be a stochastic event (see *Materials and Methods*). Although the half-lives of the reporter enzymes and their mRNAs in cone photoreceptors are unknown, both AP and β-gal accumulate to high level and are therefore relatively stable in a wide variety of transfected cell types (18, 19). If we take 5 days as a rough estimate of X, then the $t_{1/2}$ for switching is predicted to be 12 days. If some or all of the double-labeled cells arise from stable simultaneous expression of the two reporters rather than from switching between reporters, then the $t_{1/2}$ for switching among the single-labeled cells would be even greater than indicated by the preceding calculation. This estimated stability is far greater than the 15- to 80-minute switching times calculated for the β- and γ-globin genes in erythroid cells at the developmental stage when both are expressed (20). However, this estimated stability is less than that required to account for the uniformity of spectral sensitivity among cones in trichromatic primate retinae (3, 4), suggesting either that trichromatic primates have evolved mechanisms for increasing the stability of transcriptional complexes or that cis-acting DNA sequences outside of the minimal LCR fragment used here are important for stability.

An uncontrolled variable in the present experiment is the possible influence of the PGK-*neo* and HSV TK genes, which reside distal to the visual pigment-reporter genes. Although the direction of transcription of the PGK-*neo* and HSV TK genes is away from the visual pigment transgenes, precluding direct interference from convergent transcription, the possibility remains that unanticipated effects on chromatin structure and/or interference with LCR function could alter the expression pattern of the linked visual pigment reporters. Effects of this type have been inferred in several instances in which the phenotypes of different *neo* insertions in the same gene have been compared (21) or in which the phenotypes of a *neo* gene insertion has been compared with an inactivating point mutation (22) or a deletion (23). Thus, the present experiments indicate that cis-acting sequences alone can generate a mutually exclusive pattern of green and red visual pigment gene expression in a mammal that carries only a single X-linked visual pigment gene, but they leave open the exact mechanism by which this occurs.

DISCUSSION

The observations reported here have far-ranging implications for understanding the evolution, development, and function of the human visual system. In the paragraphs that follow, we interpret these observations in the context of current evidence pertaining to the evolution of trichromacy in primates, the type and specificity of synaptic connections within the retina, and the genetics of anomalous color vision in humans.

Consider an ancestral primate population in which sequence polymorphism in a single X-linked visual pigment gene produces variation in the spectral sensitivities of the encoded visual pigments, a situation observed in many present-day New World primates (1, 24). The human red and green visual pigment gene array could have arisen within this population from an unequal recombination event between X chromosomes carrying different visual pigment alleles; such a recombination event would have duplicated the transcription unit but not the LCR (Fig. 3). The data presented here predicts that this duplication would have immediately generated two classes of cones expressing predominantly or exclusively one or the other of the X-linked visual pigment genes. Both males and females carrying the duplication would very likely have good trichromatic color vision given the excellent trichromatic color vision observed in female New World monkeys that are heterozygous

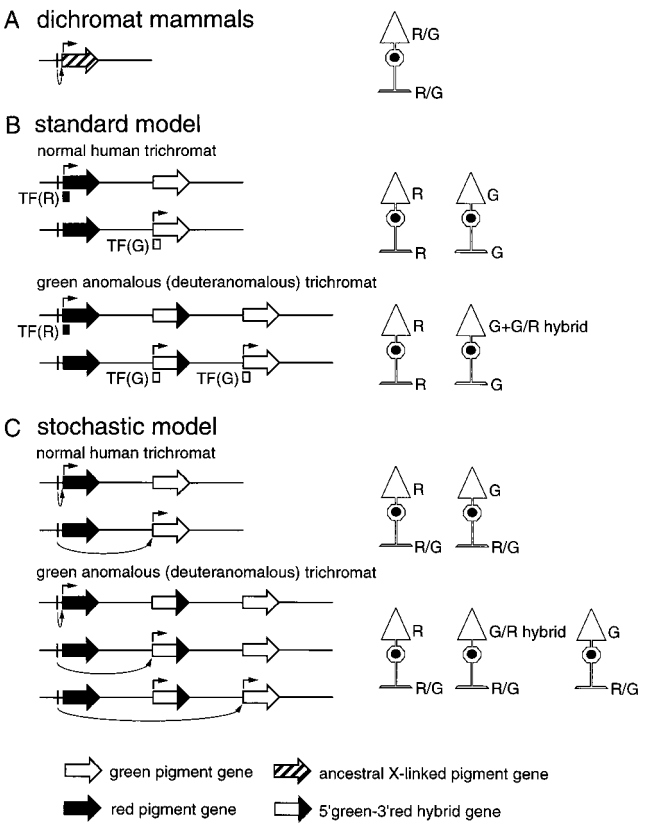

FIG. 3. Models of visual pigment gene transcription (*Left*) and the resulting visual pigment content and synaptic specificity of cones (*Right*). Individual visual pigment gene transcription units are represented by large rightward arrows as indicated in the key at the bottom. The LCR is shown as a thin vertical bar to the left of the visual pigment array, and hypothesized interactions between the LCR and individual visual pigment gene promoters are shown as curved arrows below the DNA. Transcriptional activation is represented by a rightward arrow above the indicated promoter region. The schematic diagrams of cone photoreceptors (*Right*) show the outer segment (top), a cytoplasm and nucleus (center), and a pedicle/synaptic region (bottom). The identity of the visual pigment within the outer segment and the specificities, if any, of the synaptic region are indicated adjacent to those structures. (*A*) In dichromat mammals, a single X-linked visual pigment gene is expressed in a single class of cone photoreceptors. The LCR is presumed to act on the promotor to activate transcription. (*B*) The standard model in which red-vs.-green visual pigment transcription is controlled by cell type-specific transcriptional regulatory proteins, illustrated arbitrarily as transcriptional activators, TF(R) and TF(G), present in red and green cones, respectively. The function of the LCR in the standard model is not defined but could involve pairing with promoters and/or altering the chromatin structure in and around the visual pigment gene array (39, 40). The standard model allows coordinate regulation of visual pigment type and synaptic specificity (right), and therefore red and green cones are shown with both different pigment content and synaptic specificity. (*C*) The stochastic model in which a selective interaction between the LCR and one of the visual pigment gene promoters activates transcription exclusively from that gene. Red and green cones are distinguished only by pigment content, not by synaptic specificity. *B* and *C* compare the standard and stochastic models for a color normal trichromat and a deuteranomalous trichromat who carries a red pigment gene, a 5′ green–3′ red hybrid gene, and a normal green pigment gene. In the standard model, transcription from the two green promoters could occur together in the same green cone; we note, however, that more elaborate versions of the standard model—involving an interaction between the LCR and individual promoters—might limit expression in each green cone to a single green pigment gene.

for X-linked visual pigment alleles encoding spectrally distinct visual pigments (1, 24). In the retinae of these heterozygous females, the mosaic of cones containing different X-linked visual pigments is generated by random X chromosome inactivation. The stochastic model thus provides an immediate selective advantage in both males and females that could maintain the duplication event in the gene pool.

The stochastic model in its simplest form makes the strong prediction that red and green cones are not intrinsically different from one another in synaptic specificity (Fig. 3). If correct, and if we do not invoke Hebbian mechanisms within the retina, then this idea would imply that red–green chromatic opponency of the center-surround type, which is commonly seen in ganglion cells of trichromatic primates (25, 26), simply evolved from center-surround spatial opponency by the random division of a formerly uniform population of cones into two spectrally distinct populations. The variability observed among red–green color opponent ganglion cell responses (25, 26) is consistent with this hypothesis. For red–green opponent ganglion cells near the fovea (midget ganglion cells), color opponency may simply reflect the fact that the receptive field center receives input from a single cone and the receptive field surround receives input from multiple cones, predicted by the stochastic model to be a random mixture of equivalently labeled red and green types (27, 28). By contrast, there is good evidence that the yellow–blue opponent pathway is formed by intrinsic and evolutionarily conserved differences between blue cones and the ancestral red/green cones in dichromat mammals or blue cones and equivilently labeled (and therefore summed) red and green cones in trichromatic primates (29). If ganglion cells could be shown to distinguish red from green inputs in selecting their synaptic connections, that would either negate the simple form of the stochastic model or require the participation of Hebbian mechanisms within the retina.

The stochastic model also bears on the mechanism of inherited variation in human red–green color vision, especially that associated with the addition of a 5′ green–3′ red hybrid gene to the visual pigment gene array. In the Caucasian gene pool, ≈5% of X chromosomes are of this type and are responsible for deuteranomalous trichromacy (30–32). In these arrays, the 5′ green–3′ red hybrid gene codes for a visual pigment with anomalous spectral sensitivity (33, 34), but whether this anomalous pigment (*i*) simply replaces the normal green pigment, (*ii*) is present in cones as a mixture with the normal green pigment, or (*iii*) is present in a subset of green cones is unknown. In its simplest form, the standard model predicts that differences in cis-acting DNA sequences adjacent to each transcription unit determine whether expression occurs in red or green cones. Assuming that these sequences are near the 5′ end of the transcription unit, as illustrated in Fig. 3*B*, this model predicts that each green cone in the deuteranomalous retina has the potential to express a mixture of normal and anomalous green pigment genes, although more elaborate versions of the standard model can be envisioned in which expression is limited to only a single visual pigment gene. By contrast, the stochastic model requires that each green cone express only a single visual pigment gene, implying that if both normal and anomalous green pigments are present in the retina, then they reside in different cones (Fig. 3*C*). Current data on expression of different green pigment genes suggests that the ratio of the normal to anomalous green pigment within individual cones (in the simplest form of the standard model) or the ratio of normal to anomalous green cones (in more elaborate versions of the standard model or in the stochastic model) will be highly skewed (15–17).

Finally, the observations reported here reveal more fully the significance of the X linkage of visual pigment genes in primate color vision. As noted previously, the retinal mosaicism produced by random X inactivation permits trichromatic color vision among heterozygous female primates in those species with a single polymorphic X-linked visual pigment gene (1, 24). In primates with more than one X-linked visual pigment gene, the stochastic model described here accounts for the existence of cones with mutually exclusive visual pigment expression. However, this mechanism can only be effective if, in each cone, only a single visual pigment gene array is present or available for expression, a condition that is fulfilled by hemizygosity in males and X inactivation in females, respectively.

The authors thank Drs. Janet Rossant and Se-jin Lee for embryonic stem cells; Drs. Yuji Mishina and Richard Behringer for the PGK-*neo*/HSV TK plasmid; Drs. Se-jin Lee, Randall Reed, Amir Rattner, and Joy Yang for helpful discussions; and Drs. Amir Rattner and Randall Reed for comments on the manuscript. This work was supported by the Howard Hughes Medical Institute and the National Eye Institute (National Institutes of Health).

1. Jacobs, G. H. (1993) *Biol. Rev.* **68,** 413–471.
2. Rushton, W. A. H. (1972) *J. Physiol. (London)* **220,** 1–31.
3. Dartnall, H. J. A., Bowmaker. J. K. & Mollon, J. D. (1983) *Proc. R. Soc. London Ser. B* **220,** 115–130.
4. Schnapf, J. L., Kraft, T. W. & Baylor, D. A. (1987) *Nature (London)* **325,** 439–441.
5. Nathans, J., Davenport, C. M., Maumenee, I. H., Lewis, R. A., Hejtmancik, J. F., Litt, M., Lovrien, E., Weleber, R., Bachynski, B., Zwas, F., *et al.* (1989) *Science* **245,** 831–838.
6. Wang, Y., Macke, J. P., Merbs, S. L., Klaunberg, B., Bennett, J., Zack, D., Gearhart, J. & Nathans, J. (1992) *Neuron* **9,** 429–440.
7. Chiu, M. I. & Nathans, J. (1994) *J. Neurosci.* **14,** 3426–3436.
8. Berger, J., Garattini, E., Hua, J.-C. & Udenfriend, S. (1987) *Proc. Natl. Acad. Sci. USA* **84,** 695–698.
9. Peschon, J. J., Behringer, R. R., Brinster, R. L. & Palmiter, R. D. (1987) *Proc. Natl. Acad. Sci. USA* **84,** 5316–5319.
10. Soriano, P., Montgomery, C., Geske, R. & Bradley, A. (1991) *Cell* **64,** 693–702.
11. Thomas, K. R. & Capecchi, M. R. (1987) *Cell* **51,** 503–512.
12. Mansour, S. L., Thomas, K. R. & Capecchi, M. R. (1988) *Nature (London)* **336,** 348–352.
13. Zack, D. J., Bennett, J., Wang, Y., Davenport, C., Klaunberg, B., Gearhart, J. & Nathans, J. (1991) *Neuron* **6,** 187–199.
14. Lem, J., Applebury, M. L., Falk, J. D., Flannery, J. G. & Simon, M. I. (1991) *Neuron* **6,** 201–210.
15. Winderickx, J., Battisti, L., Motulsky, A. & Deeb, S. S. (1992) *Proc. Natl. Acad. Sci. USA* **89,** 9710–9714.
16. Yamaguchi, T., Motulsky, A. & Deeb, S. S. (1997) *Hum. Mol. Genet.* **6,** 981–990.
17. Sjoberg, S. A., Neitz, M., Balding, S. D. & Neitz, J. (1998) *Vision Res.* **38,** 3213–3219.
18. Hall, C. V., Jacob, P. E., Ringold, G. M. & Lee, F. (1983) *J. Mol. Appl. Genet.* **2,** 101–109.
19. Henthorn, P., Zervos, P., Raducha, M., Harris, H. & Kadesch, T. (1988) *Proc. Natl. Acad. Sci. USA* **85,** 6342–6346.
20. Wijgerde, M., Grosveld, F. & Fraser, P. (1995) *Nature (London)* **377,** 209–213.
21. Olson, E. N., Arnold, H.-H., Rigby, P. W. J. & Wold, B. J. (1996) *Cell* **85,** 1–4.
22. Ramirez-Solis, R., Zheng, H., Whiting, J., Krumlauf, R. & Bradley, A. (1993) *Cell* **73,** 279–294.
23. Fiering, S., Epner, E., Robinson, K., Zhuang, Y., Telling, A., Hu, M., Martin, D. I. K., Enver, T., Ley, T. J. & Groudine, M. (1995) *Genes Dev.* **9,** 2203–2213.
24. Jacobs, G. H. (1998) *Invest. Ophthalomol. Visual Sci.* **39,** 2205–2216.
25. DeMonasterio, F. M. & Gouras, P. (1975) *J. Physiol. (London)* **251,** 167–195.
26. Zrenner, E., Abramov, I., Akita, M., Cowey, A., Livingstone, M. & Valberg, A. (1990) in *Visual Perception: the Neurophysiological Foundations,* eds. Spillman, L. & Werner, J. S. (Academic, New York), pp. 163–204.
27. Lennie, P., Haake, P. W. & Williams, D. R. (1991) in *Computational Models of Visual Processing*, eds. Landy, M. S. & Movshon, J. A. (M.I.T. Press, Cambridge, MA), pp. 71–82.
28. Masland, R. H. (1996) *Science* **271,** 616–617.

29. Dacey, D. M. & Lee, B. B. (1994) *Nature (London)* **367,** 731–735.
30. Pokorny, J., Smith, V. C., Verriest, G. & Pinckers, A. J. L. G. (1979) *Congenital and Acquired Color Vision Defects* (Grune & Stratton, New York).
31. Nathans, J., Piantanida, T. P., Eddy, R. L., Shows, T. B. & Hogness, D. S. (1986) *Science* **232,** 203–210.
32. Deeb, S. S., Lindsey, D. T., Sanocki, E., Winderickx, J., Teller, D. Y. & Motulsky, A. G. (1992) *Am. J. Hum. Genet.* **51,** 687–700.
33. Merbs, S. L. & Nathans, J. (1992) *Science* **258,** 464–466.
34. Asenjo, A. B., Rim, J. & Oprian, D. D. (1994) *Neuron* **12**, 1131–1138.
35. Braun, R. E., Lo, D., Pinkert, C. A., Widera, G., Flavell, R. A., Palmiter, R. D. & Brinster, R. L. (1990) *Biol. Reprod.* **43,** 684–693.
36. Nathans, J., Thomas, D. & Hogness, D. S. (1986) *Science* **232,** 193–202.
37. Vollrath, D., Nathans, J. & Davis, R. W. (1988) *Science* **240,** 1669–1671.
38. Feil, R., Aubourg, P., Helig, R. & Mandel, J. L. (1990) *Genomics* **6,** 367–373.
39. Blackwood, E. M. & Kadonaga, J. T. (1998) *Science* **281,** 60–63.
40. Higgs, D. R. (1998) *Cell* **95,** 299–302.